Effects of bound electrons and radiation on shock Hugoniot

Madhusmita Das and S. V. G. Menon*
Theoretical Physics Division, Bhabha Atomic Research Centre, Mumbai 400085, India
(Received 14 July 2008; revised manuscript received 16 November 2008; published 29 January 2009)

Hydrodynamic flow of materials, initiated by shock waves, is determined by their equation of state (EOS). For comparatively weak shocks, the zero-temperature isotherm and thermal motion of ions, mainly, determine the EOS. However, in processes involving high energy density, as in inertial confinement fusion, astrophysical phenomena, nuclear explosion, etc., very strong shocks ($P>$few megabars, $T>$few eV) are encountered. Such shocks give rise to many thermal effects leading to dissociation of molecules, ionization of electrons, radiation emission, etc., in addition to the quantum-mechanical pressure ionization in materials. Therefore, hydrodynamics due to strong shocks crucially depend on the behavior of electrons and the radiation emitted by the electrons. This paper aims at developing a simple but quantitative model of electronic binding in plasmas and its effects on compressibility of materials. An improved version of the screened hydrogenic model is developed for this purpose. The effect of radiation emission is incorporated using Stefan-Boltzmann law. The Hugoniot of various elements such as Al, Be, Fe, etc., are, then, computed. These are in excellent agreement with those obtained using sophisticated self-consistent field calculations, and the oscillations in Hugoniot are shown to be due to ionization of electrons from different shells. Shell effects are also reflected in the variation of electronic specific heat with temperature and the relation between shock velocity and fluid velocity. Further, at very high temperature and pressure, equilibration between radiation and matter increases the compressibility of materials. The limiting compression of all materials, via a strong shock, is found to be 7 unlike 4, which is the limit for free-electron gas or ideal monoatomic gas. The model reported here can be employed in lieu of Thomas-Fermi-type theories used in global EOS packages such as quotidian equation of state (QEOS).

DOI: 10.1103/PhysRevB.79.045126 PACS number(s): 62.50.Ef, 52.25.Kn, 52.25.Jm

I. INTRODUCTION

The behavior of matter under conditions of high density, pressure, and temperature is an important aspect of all astrophysical phenomena, inertial confinement fusion (ICF), planetary science, nuclear explosives, etc. All these phenomena involve compression of materials by strong shocks (pressure: $P>$few megabars, temperature: $T>$few eV). For example, pressure at the center of stars can be as high as tens or hundreds of megabars (Mbars) at temperatures of few keV. In the laboratory, conditions appropriate to high pressure or energy density are attained by launching strong shock waves. In ICF experiments, high-energy-density states are achieved where pressure is of the order of few Mbars during the implosion phase and as high as million Mbars during the explosive phase. Under such extreme conditions, matter is ionized during compression via thermal or pressure ionization and is in the form of a dense plasma. The behavior of matter in these conditions is mostly decided by the electrons present in the plasma.

The response of a material to shock is expressed in terms of the pressure-volume shock Hugoniot, which is the locus of all the thermodynamic states that can be attained via shock compression. This is obtained by solving the Rankine-Hugoniot relations along with the equation of state (EOS). The Rankine-Hugoniot relations[1] express the conservation laws of mass, momentum, and energy across the shock front and are given by

$$P_h - P_0 = \rho_0 U_s U_p, \tag{1}$$

$$V_h = V_0\left(1 - \frac{U_p}{U_s}\right), \tag{2}$$

$$E_h - E_0 = \frac{1}{2}(P_h + P_0)(V_0 - V_h), \tag{3}$$

where P_0, V_0, E_0, and P_h, V_h, E_h are, respectively, the pressure, specific volume ($\frac{1}{\rho}$), and specific energy corresponding to the undisturbed medium and shocked medium. ρ_0 and ρ are, respectively, the densities of the material before and after shock traversal. U_s is the shock velocity and U_p represents the particle velocity behind the shock. This set of three equations in five variables can be solved with the addition of the EOS of the material if one of these variables is treated as independent. The complete EOS, which relates the various thermodynamic parameters of the medium under equilibrium condition, is expressed in terms of temperature T as[2]

$$P = P(\rho, T),$$

$$E = E(\rho, T). \tag{4}$$

It is noted that for most of the systems, T can be eliminated and the EOS can be expressed in incomplete form, as in the example of ideal gas $P=(\gamma-1)\rho E$, where γ is the specific-heat ratio. In this case, the limiting value of compression ratio, defined as $\eta=\rho/\rho_0$, that can be achieved by a single shock is found, by solving the above set of equations, as[1]

$$\eta_{\text{limit}} = \frac{\gamma+1}{\gamma-1}. \tag{5}$$

At high temperatures attained via strong shocks, it is useful to invoke the free gas model of electrons for investigating the Hugoniot, as was done very recently.[3] Free electrons be-

have as a monoatomic gas, specified by $\gamma=\frac{5}{3}$. The compression ratio that can be attained by a single shock has a limiting value $\eta_{\text{limit}}=4$. This limit arises because all the energy imparted by the shock is used up for increasing the kinetic energy of electrons rather than compressing it. However, in all materials, electrons are bound to the nuclei and matter can also be in equilibrium with radiation at very high temperatures and pressures.

In this paper, we investigate the combined consequences of these two important effects. The paper is organized as follows. Section II is devoted to determine the effect of ionization of electrons on the shock Hugoniot using the simple free gas model and, then, the screened hydrogenic model. Section III investigates the effect of radiation on shock Hugoniot. In Sec. IV, the results are given for Al in detail. The effect of binding of electrons and radiation on Be and Fe Hugoniot are also discussed. We find that pressure-density shock Hugoniot shows oscillations due to shell effect, which ultimately reaches the limiting compression $\eta_{\text{limit}}=7$ in the presence of radiation.

II. EFFECT OF ELECTRONS ON HUGONIOT

The EOS of materials can be expressed as a sum of the zero temperature, or cold ($T=0$), and thermal ($T\neq 0$) parts

$$P = P_c(\rho) + P_T(\rho,T),$$

$$E = E_c(\rho) + E_T(\rho,T). \tag{6}$$

The cold pressure and energy arise due to the zero-point lattice vibrations and the zero-temperature contribution of electrons. Since the time scales for the dynamics of electrons and ions differ significantly, the ionic and electronic parts can be decoupled as

$$P_T = P_{\text{ion}}(\rho,T) + P_{\text{el}}(\rho,T),$$

$$E_T = E_{\text{ion}}(\rho,T) + E_{\text{el}}(\rho,T). \tag{7}$$

(1) Cold and Ionic EOS. The cold contribution to the EOS is accurately determined from the scaled binding-energy model.[4] The specific energy and pressure within this model are given by

$$E_c = E_{\text{coh}}[1+\epsilon(a)],$$

$$P_c = -3kB_0\frac{\epsilon'(a)}{(1+ka)^2}, \tag{8}$$

where

$$\epsilon(a) = \frac{e^{-a}(\alpha+\beta a+\delta a^2+\mu a^3)}{(1+ka)^2},$$

$$k = \frac{l}{R_0},$$

$$l = \left[\frac{E_{\text{coh}}Am_p}{12\pi B_0 R_0}\right]^{1/2},$$

$$a = \frac{r-R_0}{l}. \tag{9}$$

Here E_{coh}, B_0, and l are, respectively, the cohesive energy of the solid bulk modulus at normal density and scale length. α,β,δ, and μ are parameters which are obtained from equilibrium conditions. R_0 is the Wigner-Seitz (WS) cell radius defined below in Eq. (12).

The ionic contribution is obtained using the mean-field theory.[5,6] The free energy in this formalism is given by

$$F_{\text{ion}} = -\kappa T\left[\frac{3}{2}\ln\left(\frac{m\kappa T}{2\pi\hbar^2}\right) + \ln V_f(V,T)\right],$$

$$V_f = 4\pi\int e^{-g(r,V)/\kappa T}r^2dr,$$

$$g(r,V) = \frac{E_c(R+r)+E_c(R-r)-2E_c(R)}{2}. \tag{10}$$

The pressure P_{ion}, entropy S_{ion}, and energy E_{ion} can be calculated from free energy as

$$P_{\text{ion}} = -\left(\frac{\partial F_{\text{ion}}}{\partial V}\right)_T,$$

$$S_{\text{ion}} = -\left(\frac{\partial F_{\text{ion}}}{\partial T}\right)_V,$$

$$E_{\text{ion}} = F_{\text{ion}} + TS_{\text{ion}}. \tag{11}$$

(2) Electronic EOS. We have adapted the average atom model (AAM) to calculate the electronic contribution to the EOS. In AAM, the volume of plasma is divided into WS cells, each containing one nucleus of atomic number Z and mass number A. There are Z number of electrons in each WS cell which ensures charge neutrality within the cell. The radius (R_0) of the WS cell is determined by the density of the material and is given by

$$V_{\text{WS}} = \frac{4}{3}\pi R_0^3 = \frac{A}{N_A\rho}, \tag{12}$$

where N_A=Avogadro's number. In the AAM, all the plasma properties are averaged over the WS cells. So, it is sufficient to calculate the electronic contribution to EOS only from a single cell. The cell can contain both bound and free electrons. The free energy and specific energy corresponding to the electronic part of EOS can be expressed as[7]

$$F_{\text{el}} = F_f(\rho,T) + F_b(\rho,T) + \Delta F_{b-f}(\rho,T),$$

$$E_{\text{el}} = E_f(\rho,T) + E_b(\rho,T) + \Delta E_{b-f}(\rho,T), \tag{13}$$

where the first two terms are the contributions from free electrons and bound electrons, respectively, and the last term is introduced to account for the effect of plasma environment on the bound electronic energy levels. This effect is called continuum lowering, which is discussed in last subsection of Sec. II.

For thermodynamic consistency, pressure is obtained from the free energy as

$$P_{\mathrm{el}} = -\left(\frac{\partial F_{\mathrm{el}}}{\partial V}\right)_T. \tag{14}$$

(i) Free-electron EOS. The free electrons in the WS cell are treated as noninteracting Fermi gas. So, the free energy and specific energy are given by[3,8]

$$F_f = C_1 V(\kappa T)^{5/2}\left[\frac{\mu}{\kappa T} I_{1/2}(\mu/\kappa T) - \frac{2}{3} I_{3/2}(\mu/\kappa T)\right], \tag{15}$$

$$E_f = \frac{C_1}{\rho}(\kappa T)^{5/2} I_{3/2}(\mu/\kappa T), \tag{16}$$

where μ is the chemical potential of the electrons and κ is Boltzmann constant. At a particular temperature, μ is determined implicitly in terms of number of free electrons N in the WS cell,[8] i.e.,

$$N = \frac{C_2}{\rho}(\kappa T)^{3/2} I_{1/2}(\mu/\kappa T). \tag{17}$$

The constants C_1 and C_2 and Fermi-Dirac integrals, $I_{3/2}$ and $I_{1/2}$, are given by

$$C_1 = \frac{4\pi(2m_e)^{3/2}}{h^3}, \tag{18}$$

$$C_2 = \frac{4\pi A(2m_e)^{3/2}}{N_A h^3}, \tag{19}$$

$$I_n(\alpha) = \frac{1}{\Gamma(n+1)}\int_0^\infty \frac{x^n}{1+e^{x-\alpha}}dx, \tag{20}$$

where $\Gamma(n+1)$ is the gamma function, m_e and h are, respectively, the electron mass and Planck constant. The numerical values of C_1 and C_2 are computed such that specific energy and pressure are in units of 10^{12} erg/gm and Mbar, respectively.

From Eq. (16), it can be seen that the free electrons behave as an ideal monoatomic gas with $\gamma=\frac{5}{3}$. However, the dependence of specific energy on temperature and, consequently, temperature on the Hugoniot is different from that of ideal gas.

(ii) Bound-electron EOS. The bound electrons have been treated extensively using the self-consistent electronic structure methods within the average atom model, including relativistic effects and the effect of plasma outside the cell boundary.[9,10] The principal effect of electron binding is to introduce oscillations in the Hugoniot arising because of the shell structure of electronic "orbits." Though varying degrees of sophistication in treating electrons give rise to important differences in the Hugoniot, the general features are quite similar.

The simplest method to incorporate electronic binding, including Coulomb repulsion, is the screened hydrogen model (SHM).[11] The calculation of screening constants has been improved by several authors.[7,12] Thus, the SHM together with schemes to incorporate thermal and pressure ionization provides a simple approach for calculating the effect of binding of electrons on high pressure EOS.[7] Earlier use of the SHM for calculating the Hugoniot[13] was based on approximate treatment of l splitting[14–16] due to angular momentum (l). The calculations reported in this paper make use of the most recent compilation of screening constants, which are based on the entire available database of ionization potentials and binding energies. More importantly, a complete treatment of l splitting is included in the data fitting procedures for obtaining the screening constants.[17]

The population of electrons among various bound levels at any finite temperature and density is obtained using Fermi-Dirac distribution and a density dependent degeneracy function. The latter is important to account for the pressure ionization,[7,18] which plays a significant role in shock compression of matter. The SHM is also a good starting point to go beyond the average atom model by introducing the number distribution of various ionic species in a plasma.[19] One of the aims in this paper is to show that SHM provides quite accurate bound energy levels and hence can be used in lieu of Thomas-Fermi model in global EOS packages such as QEOS.[20,21]

A. Screened hydrogenic model

The SHM treats the interaction between bound electrons and the nucleus in a multielectron atom by an effective Coulomb-type potential ($\frac{Z_k}{r}$). An appropriate screened charge (Z_k) is determined for each quantum state $k=(n_k,l_k)$, where n_k and l_k denote the principal and angular-momentum quantum numbers, respectively.[7,17] The screened charge takes into account the interaction of a particular electron with other electrons present in the multielectron system. The effect of this interaction is only to screen the actual charge of nucleus seen by an electron in a particular level. The effective nuclear charge for an electron, i.e., screened charge Z_k, is thus always less than the actual charge of the nucleus. The single-particle energy E_k, screened charge Z_k, and the population in the shell P_k, etc., in SHM formulation, are given by[17]

$$\varepsilon_k = -\frac{Z_k^2}{2n_k^2} + \sum_1^{K_{\max}} \sigma_{kk'} P_{k'} \frac{Z_{k'}}{n_{k'}^2}, \tag{21}$$

$$Z_k = Z - \sum_1^{K_{\max}} \sigma_{kk'}(P_{k'} - f_k \delta_{kk'}), \tag{22}$$

$$P_k = f_k D_k. \tag{23}$$

The screening coefficient $\sigma_{kk'}$ determines the strength of screening in level k by electrons in level k'.[17] D_k and f_k are, respectively, the factors determining pressure and thermal ionization.[7,18] The factor D_k represents the shell degeneracy of level k for a given density and is discussed in detail in Sec. II B. f_k gives the average occupation probability of level k at a particular temperature T. This is given by the Fermi-Dirac distribution

$$f_k = \frac{1}{1+\exp[(\epsilon_k + \Delta E_{b-f} - \mu)/\kappa T]}. \quad (24)$$

The term ΔE_{b-f}, introduced to account for the continuum lowering,[18,22] is discussed in (iii).

Total energy of the bound electrons and the orbital radius of level k are given by

$$E_b = -\sum_{1}^{K_{\max}} P_k \frac{Z_k^2}{2n_k^2}, \quad (25)$$

$$r_k = \frac{a_0}{2Z_k}[3n_k^2 - l_k(l_k+1)]; \quad a_0 = \text{Bohr radius}. \quad (26)$$

Finally, the number of free electrons in the WS cell is obtained as

$$Z_0 = Z - \sum_k f_k D_k. \quad (27)$$

For a specified density and temperature of the plasma, Z_0 is determined via a self-consistent solution of the SHM. The chemical potential μ is then found using Eq. (17) with $N = Z_0$.

B. Pressure ionization

Pressure ionization is the phenomenon of ionization of electrons due to increase in density of the material. When density is increased, the interatomic separation decreases allowing the electrons of neighboring atoms to interact strongly. Because of the strong interaction and Pauli's exclusion principle, the bound states localized near the boundary are altered to a great extent. The localized states are delocalized and a band is formed due to the broadening of energy levels and the electrons are set free. This effect is usually called pressure ionization. These free electrons give an additional contribution to pressure. The consequence of this effect is to continuously ionize the electrons such that the shell degeneracy D_k decreases gradually from $g_k = 2(2l_k+1)$ to zero. Therefore, D_k must be a function of density of the plasma and can be expressed as

$$D_k = g_k \phi_k(\rho). \quad (28)$$

A simple form for the density dependent factor ϕ_k is based on the results for the degree of ionization obtained using the Thomas-Fermi model[7]

$$\phi_k = [1 + (a r_{0k}/R_0)^b]^{-1}, \quad (29)$$

where r_{0k} is the orbital radius in free atom and a and b are adjustable constants. Another form, based on Wentzel, Kramers, and Brillouin (WKB) calculation of tunneling between bound levels, is given by[18]

$$\phi_k(\rho) = 1 - \exp\left[-2\pi\sqrt{R_0}\left(1 - \frac{r_{0k}}{R_0}\right)^2\right], \quad r_{0k} \le R_0$$
$$= 0, \quad r_{0k} > R_0.$$

We have adapted this expression as it has no free parameters and it approaches zero smoothly at the WS cell boundary.

Bound electrons are distributed in various shells within the WS cell according to Fermi-Dirac distribution, with average population f_k and shell degeneracy D_k. Therefore, the entropy of bound electrons can be written as[8]

$$S_b = -\kappa \sum D_k[f_k \log f_k + (1-f_k)\log(1-f_k)]. \quad (30)$$

As the total binding energy of bound electron is known, the free energy is given by

$$F_b = E_b - TS_b. \quad (31)$$

(iii) Continuum lowering function. The last term in Eq. (13) denotes continuum lowering. It accounts for the effect of plasma environment on the bound-electron levels. In general, electrons bound as well as free and ions outside the WS cell and free electrons inside the same cell affect the bound-electron levels significantly. We neglect the effect of outside charges and consider that the levels are influenced only by the presence of free electrons inside the same WS cell. The repulsive interaction between electrons makes a positive contribution on the bound energy levels. So the levels are shifted up in energy and in effect the continuum is lowered. There are detailed methods based on Thomas-Fermi model[22] to quantify the effect of continuum lowering. However, we have adapted a simple form,[18] where it is assumed that the ion is placed inside a uniformly charged sphere containing Z_0 free electrons. This yields

$$\Delta F_{b-f} = \frac{3}{5}\frac{Z_0 e^2}{R_0}. \quad (32)$$

The total free energy ($F_{\rm el}$) can be obtained from Eqs. (16), (31), and (32). Then pressure, calculated using Eq. (14), is given by

$$P_{\rm el} = P_f + P_b + \Delta P_{b-f}, \quad (33)$$

where

$$P_f = C_1 \frac{2}{3}(\kappa T)^{5/2} I_{3/2}(\mu/\kappa T),$$

$$P_b = -\kappa T \sum_k \log(1-f_k)\frac{\partial D_k}{\partial V},$$

$$\Delta P_{b-f} = \frac{1}{40\pi}\frac{Z_0^2 e^2}{R_0^4}.$$

III. EFFECT OF RADIATION ON HUGONIOT

At high densities and temperatures, matter exists in plasma state. The electrons in the plasma produce radiation on heating via bremsstrahlung and also reach equilibrium with the plasma via inverse bremsstrahlung and Compton scattering processes. The time scale for the equilibration of radiation with matter is generally of the order of 10^{-13} to 10^{-15} s. This time scale is negligible in comparison to the time scale of shock propagation 10^{-9} to 10^{-6} s and hence, justifies the assumption that matter exists in equilibrium with

radiation.[23] Under equilibrium condition, the energy density of radiation depends on the temperature of the material. When an intense shock is launched, the temperature becomes so high that the energy density and pressure of radiation become comparable to the internal energy and pressure of electrons, thereby affecting both the EOS and Hugoniot.

(iv) EOS of electron-radiation system. In the presence of radiation, the specific energy and pressure of electron-radiation system are given by

$$E = E_{\rm el} + E_{\rm rad},$$

$$P = P_{\rm el} + P_{\rm rad}. \tag{34}$$

Specific energy and pressure of electrons are given by Eqs. (13) and (14). The pressure and energy density of equilibrium radiation can be obtained using Stefan-Boltzmann law, which is valid as pointed out earlier. Then, the energy density of radiation is given by[24]

$$W = a(\kappa T)^4. \tag{35}$$

The value of radiation constant $a=137.999$ when κT and W are expressed in keV and 10^{12} ergs/cm^3, respectively. Specific energy and pressure of (equilibrium) radiation are given by

$$E_{\rm rad} = \frac{W}{\rho},$$

$$P_{\rm rad} = \frac{1}{3}\rho E_{\rm rad}.$$

This shows that (equilibrium) radiation will respond to shock[1] as a monoatomic gas with $\gamma=\frac{4}{3}$, where as γ for a free-electron gas is $\frac{5}{3}$. That is, the EOS for a free-electron gas is

$$P_f = \frac{2}{3}\rho E_f, \tag{36}$$

where E_f is given by Eq. (16). Thus, the EOS of the electron-radiation system becomes

$$P = \rho\left(\frac{2}{3}E_f + \frac{1}{3}E_{\rm rad}\right), \tag{37}$$

$$E = E_f + E_{\rm rad}. \tag{38}$$

Equations (16) and (35) determine the relative importance of electron pressure or radiation pressure through the temperature of the medium. Thus, while the shock-induced compressibility is given by electron pressures at low temperature, the contributions from radiation will be the determining factor at high temperatures.[24]

IV. RESULTS AND DISCUSSION

A. Thermal and pressure ionizations

Using the SHM formulation, the set of nonlinear equations are solved self-consistently for different temperatures and densities to obtain the degree of ionization. Figure 1(a) shows the thermal ionization curves of Al ($Z=13, A=27, \rho_0=2.7$ gm/cc) for different densities ($0.001\rho_0<\rho<600\rho_0$). Similarly, Fig. 1(b) shows the pressure ionization curves for Al for the temperatures in the range $[0.001<T(\text{keV})<6]$. The plateaus in these curves correspond to the ionization of different electronic shells. For Al, there are two plateaus corresponding to M and L shell ionization.

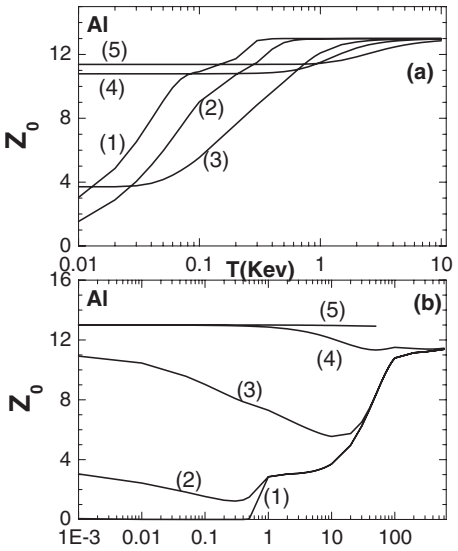

FIG. 1. (a) Ionization curves vs temperature for Al ($\rho_0=2.7$ gm/cc) at different compressions. Curves marked (1) to (5) are for $\eta=0.001$, 0.1, 10, 100, and 600, respectively. (b) Ionization curves vs compression for Al at various temperatures. Curves marked (1) to (5) are for $T=0.001$, 0.01, 0.1, 1, and 6 keV, respectively.

B. EOS energy and pressure

Figures 2(a) and 2(b) show the variation of energy and pressure with compression for Al for different temperatures in the range $[0.001<T(\text{keV})<4]$. The shell structure, evident from the plots, vanishes at very high temperature and compression as all the shells are ionized.

An important point to be noted from Fig. 2(b) is that there is no abrupt change in pressure due to ionization of the shells. This is because of the properly chosen form of the degeneracy parameter D_k, which allows continuous merging of bound levels into continuum with increasing density.

C. Shock Hugoniot and effects of radiation

For investigating the effect of electron binding on Hugoniot, Eq. (3) is to be solved in conjunction with Eq. (33) for electron pressure. This has been done for each temperature step in the interval $2.5\times10^{-5}\leq T(\text{keV})\leq 15$. The results for Al ($Z=13, A=27$) are shown in Figs. 3(a) and 3(b) without and including the effects of radiation. The Hugoniot corresponding to the free-electron gas (for $N=13$), without any electron binding, is also shown in Fig. 3(a).

The actual Hugoniot of Al lies below that of the free-electron gas. This is physically correct because binding of

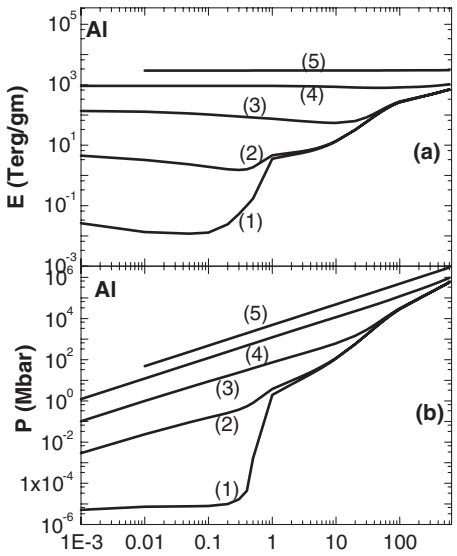

FIG. 2. (a) Pressure and (b) specific internal energy of Al vs compression at different temperatures. Curves marked (1) to (5) are for T=0.001, 0.01, 0.1, 1, and 4 keV, respectively.

electrons reduces the pressure required for compressing to same density in comparison to that in fully ionized case.

Again, the free-electron Hugoniot shows a limiting compression of 4 (η_{limit}=4) at very high pressures where as Hugoniot of Al indicates that higher compression can be achieved. This is a consequence of absorption of internal energy for ionizing the shells. However, as the shells are ionized, more and more electrons are set free. The increase in pressure due to release of more free electrons opposes compression. At some point, this opposing "force" dominates

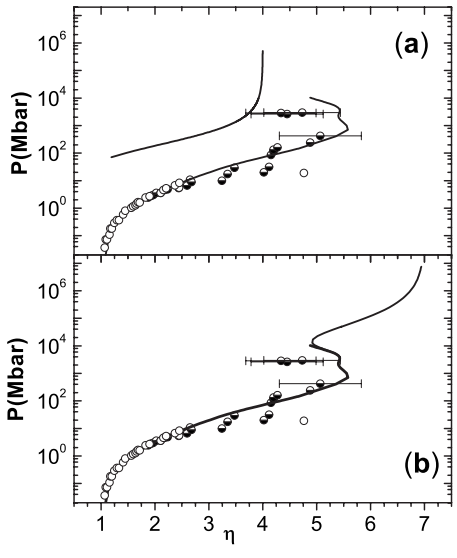

FIG. 3. (a) Hugoniot of Al vs compression. Solid line represents theoretical Hugoniot, empty circles represent low-pressure experimental data, and half-filled circles represent experimental data at high pressures. Upper curve with squares is Hugoniot for free-electron gas with 13 electrons. (b) Hugoniot in presence of radiation. Empty and half filled circles denote the experimental data (Refs. 10 and 21).

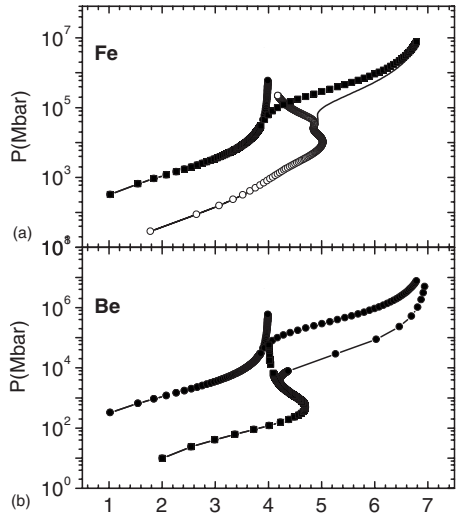

FIG. 4. (a) Line with filled circles is Hugoniot of free-electron gas (N=26), line with squares is Hugoniot of combined system of free electrons and radiation. Line with empty circles is the Hugoniot of Fe (Z=26,A=56) with electron binding and solid line is Hugoniot for Fe in the presence of radiation. (b) Same as above but for Be (Z=4,A=9).

over the amount of internal energy absorbed, thereby decreasing further compression of the material. The oscillations appearing in the Hugoniot are due to the shell ionization. At extreme pressures, the Hugoniot will join that of the free electrons. Temperature along the Hugoniot is also shown in the figure.

As seen from Fig. 3(a), the SHM is also validated against the experimental data[21] for Al. Theoretically calculated values show good agreement with the experimental data for low pressure and temperature. The experimental results for very high temperature and pressure, generally obtained from nuclear explosions, have large error bars.

The Hugoniot relation given by Eq. (3) can be solved together with Eq. (37) at different temperatures. The resulting Hugoniot for Al is shown in Fig. 3(b), which shows that equilibrium radiation affects compression after about 10^4 Mbars. This is also seen from the temperature along the Hugoniot shown in the figure. It is clear that for temperature $T>1$ keV, the radiation contributes significantly to the EOS. This is because the radiation energy density increases as fourth power of the material temperature. At temperatures where the radiation effect is quite dominant, the compressibility of the system increases because of the comparatively lower value of $\gamma=\frac{4}{3}$ for photon gas. Thus the limiting compression becomes 7 in comparison to 4 for free electrons.

For temperature (>20 eV), electron contribution becomes comparable to the cold and ionic contributions. At $T\sim150$ eV, first shell ionization takes place and around $T\sim550$ eV, second shell of Al gets ionized. At $T>1$ keV, all the shells are ionized and the system behaves as a monoatomic gas with the limiting compression of 4.

More results of calculations of Hugoniot in presence of radiation are shown in Fig. 4(a) for Fe and Fig. 4(b) for Be, respectively. As expected, the limiting compression in all cases is now 7. Plots of electron and radiation pressures

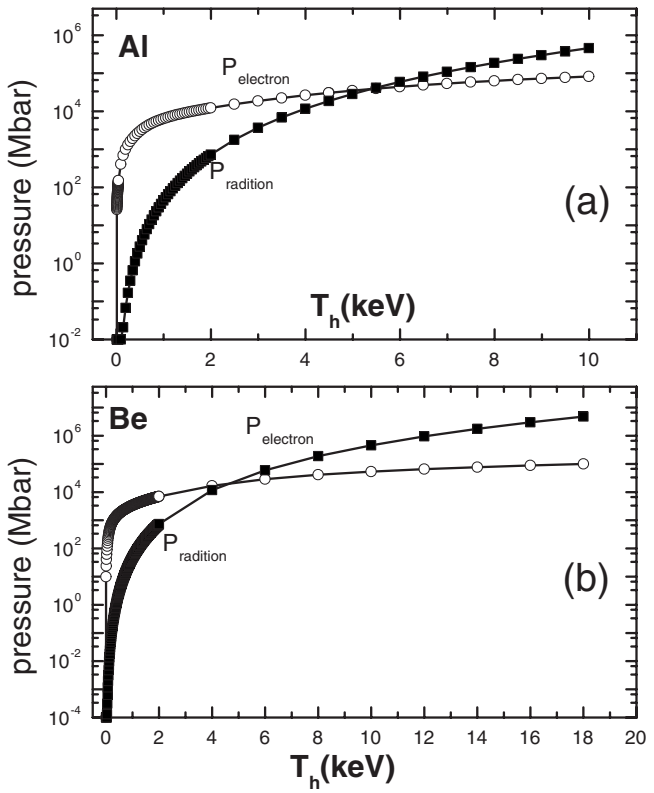

FIG. 5. (a) Line with circles is electronic part of Al EOS and line with squares is the radiative contribution to its EOS along the Hugoniot. The crossover temperature is at $T\sim 5$ keV. (b) Same as above for Be, but the crossover temperature is at $T\sim 4$ keV.

against Hugoniot temperatures are also given for Be and Al in Figs. 5(a) and 5(b), which clearly illustrate the crossover to radiation pressure at higher temperatures (~4 KeV).

Number of oscillations in the Hugoniot depends on the number of shells present in the atom. For Be ($Z=4$, $A=9$, $\rho_0=1.85$ gm/cc), there is a single oscillation, as shown in Fig. 4(b), at a temperature of 175 eV corresponding to the K-shell ionization. For Al ($Z=13$, $A=27$, $\rho_0=2.74$ gm/cc), there are two oscillations corresponding to K-shell and L-shell ionizations around 150 and 550 eV, respectively. For Be we get a maximum compression $\eta_{\text{limit}} \approx 4.6$ without radiation, while it is around 5.4 for Al. These values are in excellent agreement with more detailed and sophisticated calculations.[9] The Hugoniot for Fe ($Z=26$, $A=56$, $\rho=7.88$ gm/cc) given in Fig. 4(a) shows three oscillations due to the ionization of K,L,M shells. In Fe, the L-shell effect is more prominent than K and M shells. This is because the number of electrons in this shell is comparatively larger than in K and M shells. Hence, more amount of internal energy is absorbed, allowing a comparatively higher degree of compression.

D. Electronic specific heat

The electronic specific heat per atom at constant volume is given by

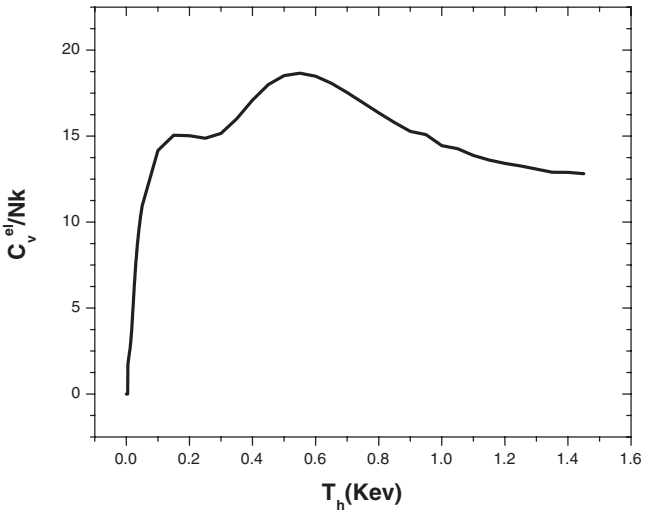

FIG. 6. Electronic specific heat of Al vs temperature along the Hugoniot. The pronounced peak at $T\sim 550$ eV is due to the "Schottky anomaly."

$$\frac{C_v^{\text{el}}}{\left(\frac{3\kappa}{2}\right)} = \left(\frac{\partial E_{\text{el}}}{\partial T}\right)_V.$$

Figure 6 shows the variation of $\frac{C_v^{\text{el}}}{(\frac{3\kappa}{2})}$ with temperature on Hugoniot for Al. This plot carries the signature of quantum shell effect. As we go along the Hugoniot, temperature increases and more number of electrons become free thereby increasing the specific heat. At a temperature around ~150 eV, corresponding to ionization of L shell, the specific-heat curve has a weak hump. As the temperature is increased further, a sharp peak appears at around ~550 eV. This peak corresponds to the ionization of the $1s$ shell which is a strongly bound level. The height of the peak in the specific-heat curve is determined by the ionization potential of this shell. Since the ionization energy of the $3s$ and $2p$ levels are not very high, their effect is not pronounced as compared to that of $1s$ and $2s$ levels. The occurrence of the pronounced peak in the specific-heat curve is called "Schottky anomaly." When all the electrons are ionized at high temperature, the system behaves as a monoatomic gas with 13 electrons and specific heat approaches the value 13 asymptotically.

E. Shock speed vs particle speed

The shock speed and particle speed behind the shock are, respectively, given by[1]

$$U_s = \sqrt{\frac{\rho_h(P_h - P_0)}{\rho_0(\rho_h - \rho_0)}},$$

$$U_p = \frac{P_h - P_0}{\rho_0 U_s}.$$

We have investigated the variation of the difference $U_s - U_p$ with particle speed U_p for Al and the results are shown in

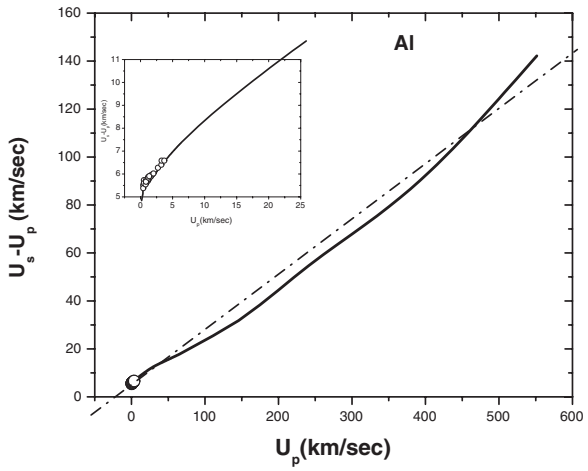

FIG. 7. Variation of $U_s - U_p$ with U_p for Al along the Hugoniot. Dotted line is a linear fit. Empty circles in inset show the experimental.

Fig. 7 together with experimental values. There is good agreement between the two sets of data. The presence of weak oscillations shows that the variation of U_s with U_p is not linear. Shell effects, which lead to the oscillations, are not pronounced because U_s vs U_p curves are not very sensitive to the material property.

V. CONCLUSION

We have shown that the SHM can accurately describe the behavior of bound electrons in a plasma. Our results show that in the intermediate temperature range $[0.02 < T(\text{keV}) < 1]$, the electrons play a significant role in deciding the compressibility of matter. At higher temperatures, it is the radiation pressure which plays the main role and this increases compressibility. We also infer the general principle: compressibility of a material depends on the available internal degrees of freedom which can absorb energy from the shock. The more the number of degrees of freedom, the more is the attainable compression. Unlike in the case of free electrons, addition of radiation and binding effects leads to higher compression at relatively lower shock pressures. This conclusion can still be improved upon by incorporating relativistic effects and the interaction between free electrons, which are important for heavier elements such as uranium.

Most of the EOS packages use Thomas-Fermi (TF) model to incorporate the effect of electrons on the EOS of materials under shock compression. As TF model is a statistical model, it does not reproduce the shell effects in the Hugoniot curves. However, the shell effect can be seen clearly when the electron binding and pressure ionization are accounted correctly. Though there are self-consistent field methods, which give results close to the experimental values, these are generally not suitable for in-line calculation. The model we have presented gives almost the same accuracy as offered by self-consistent field calculations. The accuracy attained can be improved further by refining pressure ionization scheme. Finally we note that the SHM, with explicit treatment of l splitting as done in this paper, can be used in lieu of TF model in global EOS packages such as QEOS.

ACKNOWLEDGMENTS

We are grateful to Chandrani Bhattacharya, Theoretical Physics Division, BARC, for useful discussions throughout the course of this work.

*msdas@barc.gov.in

[1] Ya. B. Zeldovich and Yu. P. Raiser, *Physics of Shock Waves and High Temperature Hydrodynamic Phenomena* (Academic, New York, 1966), Vol. 1.
[2] S. Eliezer, A. Ghatak, H. Hora, and E. Teller, *An Introduction to Equation of State: Theory and Applications* (Cambridge University Press, New York, 1986).
[3] W. J. Nellis, J. Appl. Phys. **94**, 272 (2003).
[4] Chandrani Bhattacharya and M. K. Srivastava, J. Appl. Phys. **102**, 1 (2007).
[5] Chandrani Bhattacharya and S. V. G. Menon (unpublished).
[6] Y. Wang, Phys. Rev. B **61**, R11863 (2000).
[7] G. B. Zimmerman and R. M. More, J. Quant. Spectrosc. Radiat. Transf. **23**, 517 (1980).
[8] K. Huang, *Statistical Mechanics* (Wiley Eastern Limited, New Delhi, 1975).
[9] B. F. Rozsnyai, J. R. Albritton, D. A. Young, V. N. Sonnard, and D. A. Liberman, Phys. Lett. A **291**, 226 (2001).
[10] J. C. Pain, High Energy Density Phys. **3**, 204 (2007).
[11] H. Mayer, Los Alamos Scientific Laboratory Report No. LA-647, 1947 (unpublished).
[12] R. Marchand, S. Caille, and Y. T. Lee, J. Quant. Spectrosc. Radiat. Transf. **43**, 149 (1990).
[13] S. A. Bel'kov, S. V. Bondarenko, and E. I. Mitrofanov, Quantum Electron. **30**, 963 (2000).
[14] F. Perrot, Phys. Scr. **39**, 332 (1989).
[15] A. Rickert and J. Meyer-Ter-Vehn, Laser Part. Beams **8**, 722 (1990).
[16] S. A. Bel'kov, P. D. Gasparyan, Yu. K. Kochubei, and E. I. Mitrofanov, J. Exp. Theor. Phys. **84**, 272 (1997).
[17] G. Faussurier, C. Blancard, and A. Decoster, J. Quant. Spectrosc. Radiat. Transf. **58**, 233 (1997).
[18] R. C. Mancini and C. F. Fontan, J. Quant. Spectrosc. Radiat. Transf. **34**, 115 (1985).
[19] G. Faussurier, C. Blancard, and A. Decoster, Phys. Rev. E **56**, 3474 (1997).
[20] R. M. More, K. H. Warrren, D. A. Young, and G. B. Zimmerman, Phys. Fluids **31**, 3059 (1988).
[21] David A. Young and Ellen M. Corey, J. Appl. Phys. **78**, 3748 (1995).
[22] J. C. Stewart and K. D. Pyatt, Astrophys. J. **144**, 1203 (1966).
[23] W. J. Nellis, Rep. Prog. Phys. **69**, 1479 (2006).
[24] R. G. Sachs, Phys. Rev. **69**, 514 (1946).